SLAC-PUB-4728
September 1988
(A)

Distribution of Induced Activity in Tungsten Targets*

R. J. DONAHUE AND W. R. NELSON

Stanford Linear Accelerator Center
Stanford, California 94309

Abstract

Estimates are made of the induced activity created during high-energy electron showers in tungsten, using the EGS4 code. Photon track lengths, neutron yields and spatial profiles of the induced activity are presented.

Presented at the Health Physics Society Annual Meeting,
Boston, MA., July 4–8, 1988

---

* Work supported by the US Department of Energy under contract DE-AC03-76SF00515

Introduction

The induced activity produced in high-energy electron accelerator beam devices (e.g., targets, stoppers, collimators, etc.) is not uniform. Instead, it follows somewhat the electromagnetic shower profile. The majority of the activity is created by photonuclear reactions with target nuclei, primarily through excitation of the giant resonance. This note begins an EGS4 Monte Carlo investigation of this problem by examining the induced activity profile in tungsten targets as a benchmark.

Giant Resonance Neutron Production

High-energy photons are created during the electromagnetic cascade. Although only a minor process in the cascade itself, these photons exhibit a large photonuclear peak around the giant resonance of threshold energies ranging from about 6 MeV for heavy target nuclei to 25 MeV for light materials. This is nicely shown in Fig. 1 , where various photon interaction processes are given. Three photonuclear (as oppossed to photoatomic) cross sections are shown: giant resonance, quasi-deuteron, and pion production. It has been estimated[1] that giant resonance reactions occur 100 to 1000 times more frequently than the other photonuclear reactions.

When a photon interacts with a nucleus via the giant resonance, it may knock out one or more charged and/or uncharged nucleons. Typical giant resonance reactions are (γ ,n), (γ ,2n), (γ, p), (γ ,pn), etc. While it is true that these nucleons may then interact with other nuclei, creating additional activity in the target, the majority of the induced activity is assumed to be created in the initial interaction. For some key isotopes, however, this may not be true. Based on this assumption, if one were to find a way of scoring (via Monte Carlo) the yields and location of giant resonance neutron production, then a spatial distribution of the induced activity could be estimated.

Before the spatial distribution of the activity is calculated, two methods of verifying our model are used: (1) comparison of the photon track lengths, and (2) comparison of neutron yields.

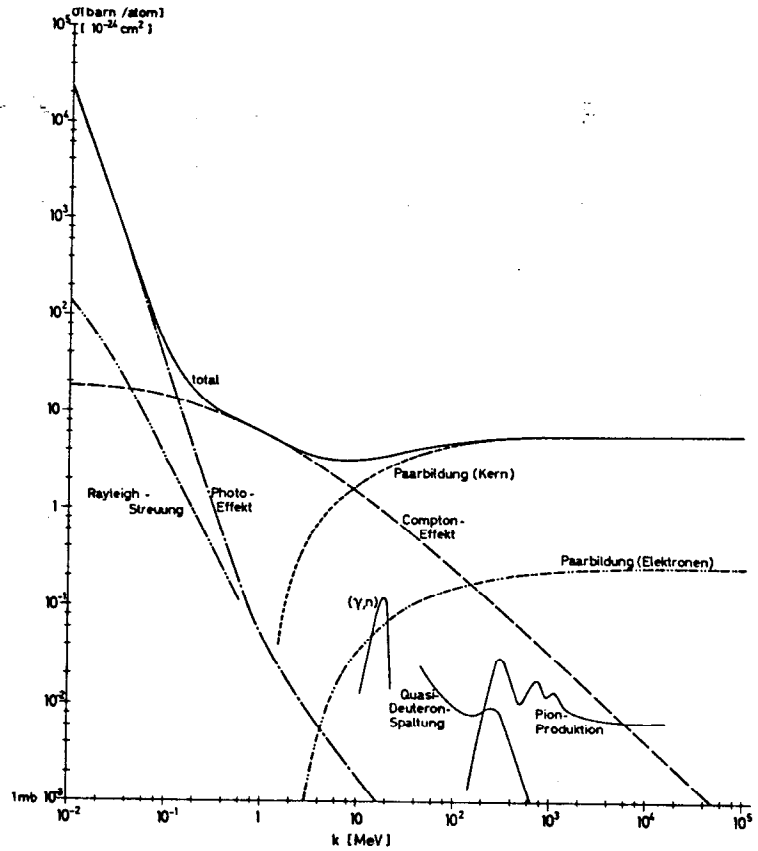

Figure 1. Photon cross sections as a function of energy (taken from Freytag[2]).

Differential Photon Track Length

The giant resonance neutron yield can be calculated from

$$Y_{GRN} = C \int_{E_{th}}^{E_0} \sigma(k) \frac{dl}{dk} dk \qquad (1)$$

where:

Y_{GRN}= giant resonance neutron yield (n/e$^-$)

σ= giant resonance cross section (mb)

$\frac{dl}{dk}$= differential photon track length (r.l./MeV)

C= constant (1/r.l.-mb.)

E_0= incident electron energy (MeV)

E_{th}= kinematic threshold energy (MeV)

The differential photon track length is the distance travelled by photons with an energy which lies between k and k+dk. Since photons interact catastrophically (as opposed to a continuous energy loss for charged particles) The track lengths may be easily scored as a function of energy.

The EGS4 code[3] was used to calculate the differential photon track length in tungsten for various incident electron energies. The track length results were compared against:

- Approximation A of Shower Theory[4] .

$$\frac{dl}{dk} = 0.572\frac{E_0}{k^2}$$

- Clement and Kessler Formula (Cl63).

$$\frac{dl}{dk} = 0.964\frac{u}{k}[-\ln(1-u^2) + 0.686u^2 - 0.5u^4]^{-1}$$

- Monte Carlo results of Berger and Seltzer[5] using the ETRAN code.

Figure 2 , compares track length results for 50 GeV electrons incident on a thick (5.95 cm. = 17 r.l.) tungsten target.

The comparison shows good agreement with EGS4 except at energies close to the incident electron energy. As the energy approaches E_0, both the Clement and Kessler formula and the EGS4 results begin to fall sharply. The Approximation A expression, of course, does not account for the kinematic limit and simply falls off as $1/k^2$.

Figure 3 shows a comparison of the differential photon track length calculated by EGS4 and by ETRAN [5] . The calculation was performed for two different incident electron energies (30 and 60 MeV) and various thicknesses (r_0) of tungsten.

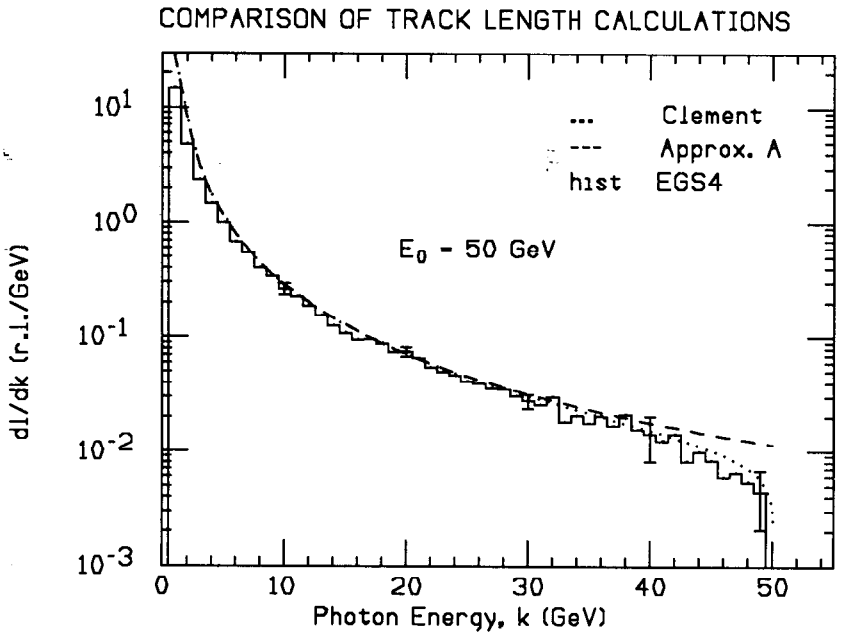

Figure 2. Photon track length comparisons as a function of photon energy.

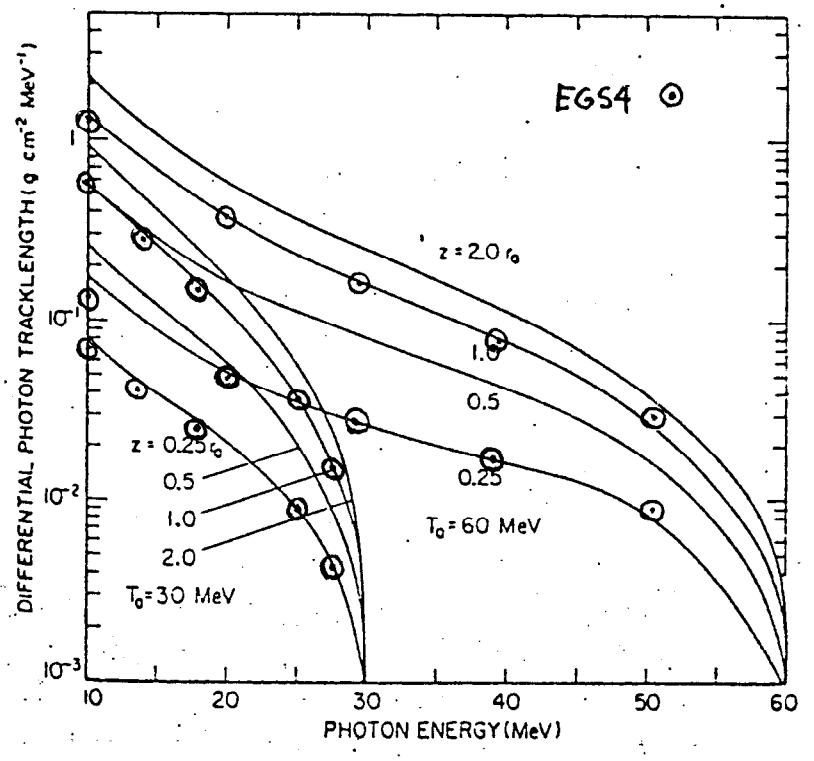

Figure 3. EGS4 and ETRAN photon track length comparisons.

As discussed previously, neutron yields are calculated using Eqn. 1. The giant resonance cross sections for tungsten are taken from Berman [6] and are input as data

for different energy groups in the EGS4 User Code. For purposes of Monte Carlo integration, the cross sections are input in a fine enough energy mesh such that linear interpolation is valid for photons of intermediate energies.

Neutron Yields

Figure 4 shows a comparison of neutron yields (n/e^-) for incident electron energies varying from 10-34 MeV in a one radiation length tantalum target. Tantalum was used for the comparison since these yields were available, and they were not available for tungsten. The EGS4 data has been plotted on top of the experimental data of Barber and George[7]The EGS4 statistical error bars are smaller than the data points shown. It should be pointed out that the thickness used by Barber and George was quoted as 6.2 g cm^{-2} (and 0.98 r.l.). Using a density of 16.6 g cm^{-3}, the thickness becomes 0.374 cm, which was used in the EGS4 calculation. This turns out to be 0.91 r.l. as calculated by EGS4. If EGS4 were run with a 7% thicker target the results would agree rather well.

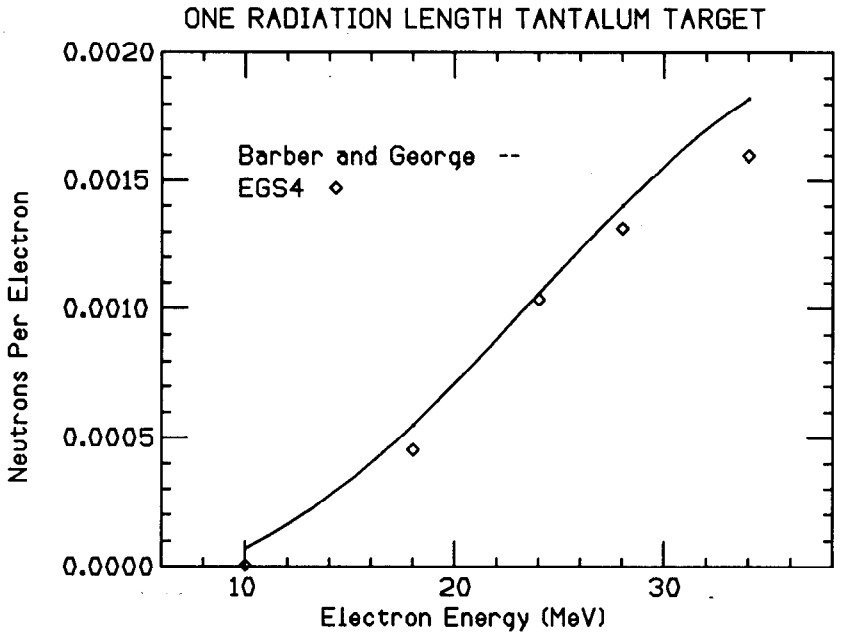

Figure 4. Neutron yield comparison.

Spatial Distribution of Activity

As discussed previously, scoring how often and where the giant resonance neutrons are produced provides an estimate of the yield and spatial distribution of the induced activity in the target.

Initial and final photon track positions in the shower are determined by EGS4. The activity is assumed to be produced randomly along the track, since the photoneutron cross section is several orders of magnitude smaller than the usual photon cross sections. Since only the relative production is of interest here, as opposed to the absolute amount of activity produced, all photons are assumed to undergo giant resonance neutron production. This is also only true if the photon energy is within the resonance energy limit, otherwise it is discarded. The total amount of activity produced here is therefore high by the ratio of $\sigma_{total}/\sigma_{GRN}$ at a given energy. This ratio is approx. 100 - 1000. This biasing is done to improve the statistics.

The production of activity is also statistically biased (i.e., weighted by the cross section) such that photons with an energy close to the peak of the giant resonance are more likely to interact and produce activity than photons of higher or lower energy about the peak.

The giant resonance cross sections from Berman are for natural tungsten which consists primarily of 5 isotopes; ^{180}W (0.14 %), ^{182}W (26.41 %), ^{183}W (14.4 %), ^{184}W (30.64 %), and ^{186}W (28.41 %). The most important induced isotopes, in terms of gamma activity produced in a thick natural tungsten target, as well as their respective production modes, are listed in Table 1. Note that the first two reactions in this table both produce ^{181}W, which has a Γ of 3.3 x 10^{-17}.

Table 1. Induced radionuclide properties of a natural tungsten target.

Reaction	End Product	Half Life (days)	Γ (R/hr-m^2)*
^{182}W(γ ,n)	^{181}W		
^{183}W(γ ,2n)	^{181}W	130	3.3×10^{-17}
^{183}W(γ ,p)	^{182}Ta	115	1.7×10^{-18}
^{184}W(γ ,p)	^{183}Ta	5	3.3×10^{-18}
^{186}W(γ ,p)	^{185}Ta	0.03	1.0×10^{-18}
^{180}W(γ ,n)	^{179}W	0.021	2.5×10^{-19}

* Assumes activity is at saturation with no decay, 1 e^-/sec incident on a thick target. Normalized per MeV of incident beam energy (taken from Ref. 1).

Figure 5 , Fig. 6 and Fig. 7 show representations of the induced activity produced in a 9 cm long by 5 cm radius cylinder of tungsten. These have been produced using the EGS4 graphics package[8] . Shower theory (*e.g.*, Approximation A) tells us that the number of particles produced in a shower is directly proportional to the incident electron energy. Therefore going from 1000 incident electrons at 100 MeV/e^- to 100 incident electrons at 1 GeV/e^- will give approximately the same number of shower particles. However, the spatial profile of the induced activity changes with different incident energies because the shower profile changes. This is clearly shown in the following three figures.

Figure 8 and Fig. 9 represent the distribution of induced activity in a natural tungsten target for various incident electron beam energies. The radionuclide yield is the number of nuclides created per incident electron. The distribution is assumed to be the same for all of the end products listed in Table 1, since the reaction thresholds are very close to one another. Figure 8 shows the yield as a function of depth into the target, integrated over the radius. It is obvious that the activity is not uniformly distributed, but instead tends to follow a shower profile. The more energetic the

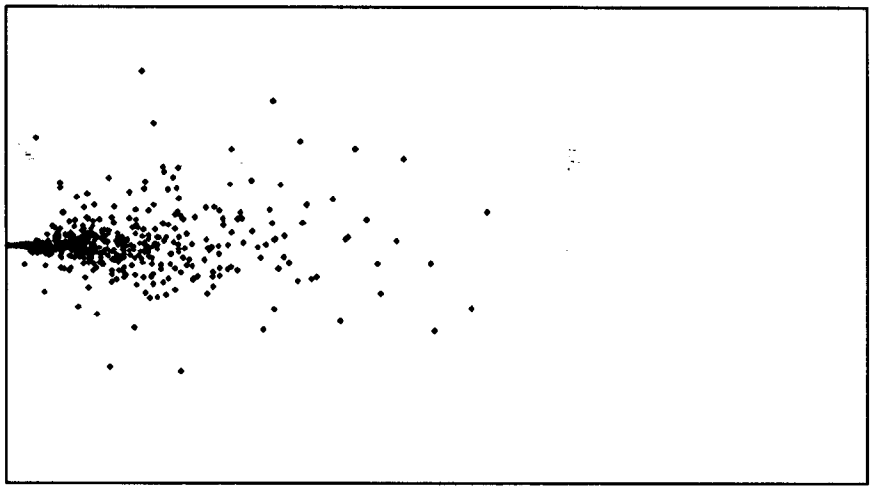

Figure 5. Activity produced by 1000 incident electrons at 100 MeV/e^-.

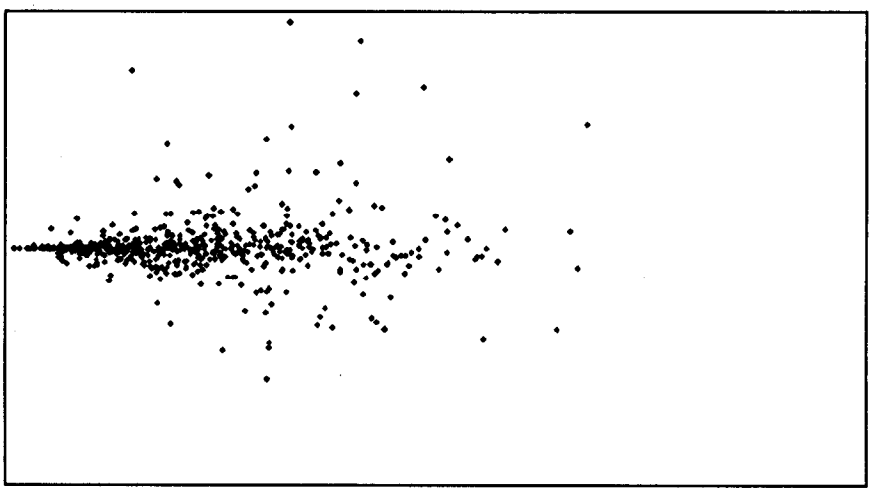

Figure 6. Activity produced by 100 incident electrons at 1 GeV/e^-.

found. Whereas in relatively low energy beams, most of the activity is produced near the front surface.

Figure 9 shows the radionuclide yield as a function of radius in the target, integrated over the depth. It can be seen that the activity is produced very tightly about the incident beam axis, dropping an order of magnitude in less than 1 centimeter radius.

Conclusion

The production of activity by high-energy electron beams can be modelled using the EGS4 code. This work has been done for only one target material (tungsten) and

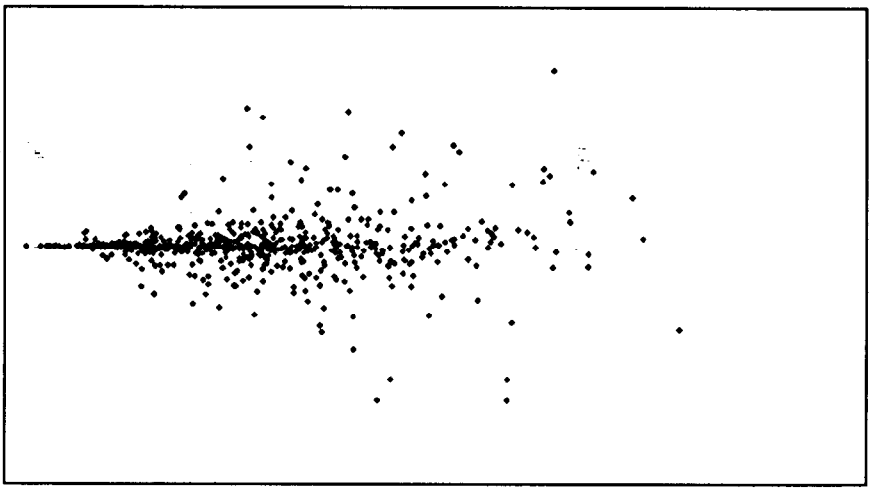

Figure 7. Activity produced by 10 incident electrons at 10 GeV/e^-.

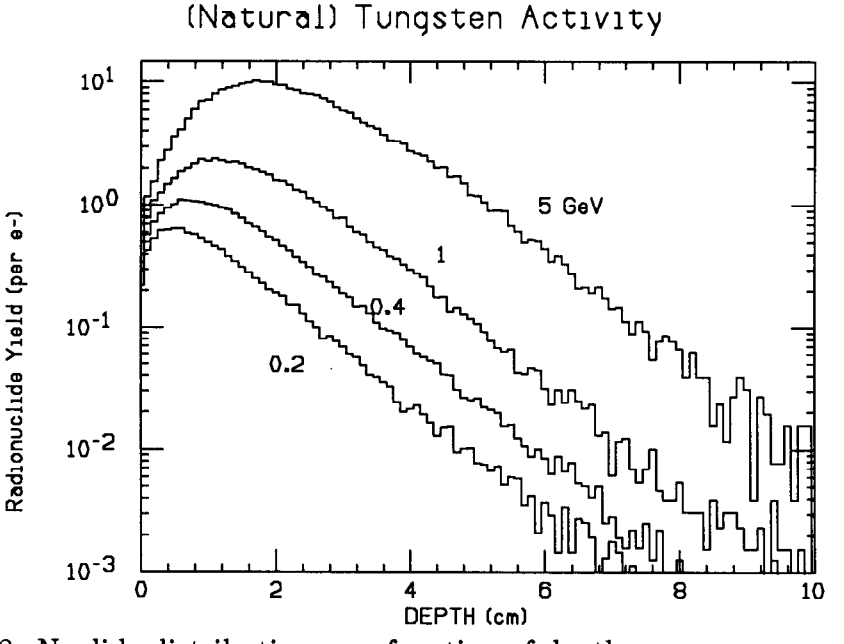

Figure 8. Nuclide distribution as a function of depth.

should be extended to include other materials such as Cu, Al, Fe and U.

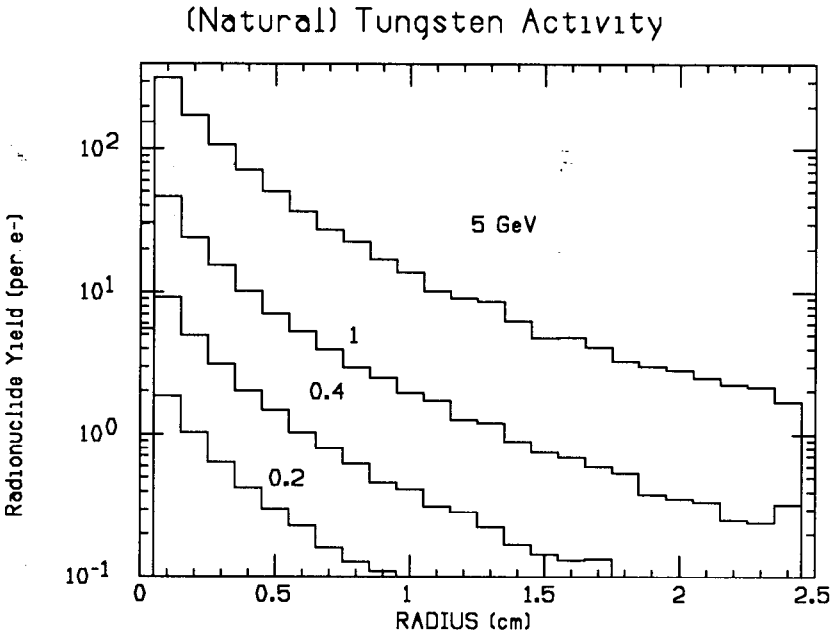

Figure 9. Nuclide distribution as a function of radius.

REFERENCES

1. M. Barbier, *Induced Activity* (North-Holland, 1969).
2. E. Freytag, *Strahlenschutz an Hochenergiebeschleunigern* (G. Braun, Karlsruhe, 1972).
3. W. R. Nelson, H. Hirayama, and D. W. O. Rogers, "The EGS4 Code System", SLAC-265 (1985).
4. B. Rossi, *High-Energy Particles* (McGraw-Hill, 1952).
5. M. Berger and S. Seltzer, "Bremsstrahlung and Photoneutrons from Thick Tungsten and Tantalum Targets", Phys. Rev. **2 (2)** (1970) 621.
6. B. L. Berman, "Atlas of Photoneutron Cross Sections Obtained With Monoenergetic Photons", UCRL-78482 (1976).
7. C. Barber and W. D. George, "Neutron Yields from Targets Bombarded by Electrons", Phys. Rev. **116 (6)** (1959) 1551.
8. R. Cowan and W. R. Nelson, "Producing EGS4 Shower Displays With Unified Graphics", SLAC-TN-87-3 (1987).